

# MODELLING OF THE TORSIONAL IR SPECTRA OF THE HSSSH, DSSSH, AND DSSSD MOLECULES

G.A. Pitsevich<sup>a</sup>, A.E. Malevich<sup>b</sup>, U.U Sapeska<sup>c</sup>, D. Kisuryna<sup>d</sup>, I.Yu. Doroshenko<sup>e</sup>

<sup>a</sup>Department of Physical Optics and Applied Informatics, Faculty of Physics, Belarusian State University, Nezavisimosti Ave., 4, 220030, Minsk, Belarus

<sup>b</sup>Department of Differential Equations and System Analysis, Faculty of Mechanics and Mathematics, Belarusian State University, Nezavisimosti Ave., 4, 220030, Minsk, Belarus

<sup>c</sup>Faculty of Physics, the University of Illinois at Chicago, 845 W Taylor St, Chicago, IL 60607, USA

<sup>d</sup>Department of Chemistry and Biochemistry, University of Maryland, College Park, MD 20742, USA

<sup>e</sup>Faculty of Physics, Taras Shevchenko National University of Kyiv, Volodymyrska str. 64/13, 01601, Kyiv, Ukraine

\*Corresponding author email: pitsevich@bsu.by (G.A. Pitsevich)

## ABSTRACT

*Equilibrium configurations of trans- and cis- conformers of the HSSSH molecule (trisulfane), as well as the vibrational spectra of both conformers, were calculated at the MP2/Aug-cc-pVTZ level of theory in the harmonic and anharmonic approximations. A more accurate analysis of torsional vibrations of thiol groups was performed by constructing 2D surfaces of a) potential energy, b) kinetic coefficients, and c) dipole moment components as functions of torsional coordinates of S-H groups. The values of b) and c) were calculated at the MP2/Aug-cc-pVTZ level of theory while the values of a) were calculated at the B3LYP/Aug-cc-pVTZ, MP2/cc-pVTZ, MP2/Aug-cc-pVTZ, MP2/cc-pVQZ, MP2/CBS(T,Q) and CCSD(T)/Aug-cc-pVTZ levels of theory. The energies of the stationary torsional states of the trisulfane molecule conformers were determined by numerically solving the vibrational Schrödinger equation of restricted dimensionality. The frequencies of torsional vibrations of S-H groups, as well as the splittings of torsional energy levels in trans- and cis-conformers due to tunneling between equivalent configurations of the molecule, were determined. The calculated values of tunneling frequencies in the ground torsional state of HSSSH and DSSSD trans-conformers ( $2.3 \cdot 10^{-22}$  and  $7.5 \cdot 10^{-29} \text{ cm}^{-1}$ , respectively) are of particular interest due to the fact that trisulfane is considered to be one of the best candidates for establishing the effect of violation of parity conservation law in chiral molecules.*

**KEYWORDS:** torsional vibrations, potential barriers, trisulfane, PES, internal rotation, conformers, DVR, HSSSH

## 1. INTRODUCTION

The trisulfane molecule (HSSSH) is the third representative in the series of higher sulfanes of the  $\text{HS}_n\text{H}$  type ( $n=1,2,3\dots$ ). Its properties are in many respects similar to those of the hydrogen trioxide molecule ( $\text{HOOOH}$ ), which is also the third representative in the series of polyoxides of the  $\text{HO}_n\text{H}$  type ( $n=1,2,3\dots$ ). Despite the fact that polyoxides are of greater practical interest in many applications than higher sulfanes, the trisulfane molecule has undoubtedly received more attention from researchers than the hydrogen trioxide molecule. Raman spectra of higher sulfanes in the liquid phase were first recorded as early as 1956 [1]. Later, higher quality IR and Raman spectra of the molecule in  $\text{CCl}_4$  and  $\text{CS}_2$  solutions were obtained in [2], where the authors also determined the normal vibrations of the molecule. The authors of [2] properly established that the most low-frequency fundamental vibration of the HSSSH molecule is the bending S-S-S vibration and calculated very accurately the values of the torsional vibrations frequencies of thiol groups. However, there is no individual consideration of trans- and cis- conformers in this work. A detailed analysis of conformational states of the molecules representing the general form  $\text{XYZYX}$  was first performed in [3]. Geometric parameters and relative energies of higher sulfanes were calculated using non-empirical quantum-chemical methods in [4]. Potential barriers to internal rotation in the HSSSH molecule were calculated by quantum chemical methods in [5]. At the end of the 1980s, a number of papers were published in which purely rotational and microwave spectra of the trisulfane molecule were recorded and analyzed in detail. Rotational spectrum of the HSSSH molecule was first revealed in [6]. In subsequent papers [7,8], the authors established the presence of the cis-conformer and determined parameters of the molecule in the ground and excited vibrational states. Later, in [9,10], absorption bands due to the rotational transitions of the trans- conformer were reliably presented, their intensity alternated as 3:1 due to the quantum effects that arise when the nuclei of hydrogen atoms exchange places. The authors of [7-10] note that performed studies did not reveal the splittings of spectral lines caused by tunneling between equivalent configurations in both conformers. It is interesting to point out that quite a long time ago [11] M. Quack began to search for a suitable chiral molecule in the spectra of which one could observe very small splittings of energy levels due to the parity breaking effect. In [12,13], M. Quack's group performed 2D PES calculations for the trisulfane molecule. According to the authors' estimations, the splitting of the ground level due to the violation of parity law in the analyzed molecule should be of the order of  $10^{-12} \text{ cm}^{-1}$ , while the ground level splitting due to tunneling should be of the order of  $10^{-23} \text{ cm}^{-1}$ . However, the last splitting value was obtained using extrapolation approaches [14,15].

Previously, we have analyzed torsional states and IR spectra of a number of molecules with similar structure:  $\text{HO}(\text{CH}_2)\text{OH}$  [16,17],  $\text{HOOH}$  [18,19],  $\text{HSOSH}$  [20,21],  $\text{HOSOH}$  [22],  $\text{C}_6\text{H}_4(\text{OH})_2$ -ortho [23],  $\text{CH}_3\text{CH}_2\text{OH}$  [24], and  $\text{CH}_3\text{OOH}$  [25]. Although the trans- conformers of all these molecules are energetically preferable to the cis- conformers, their relative energies differ significantly. The tunneling frequencies in the ground torsional states of these molecules calculated using variational methods turned out to be  $2.1 \cdot 10^{-6}$ ,  $1.0 \cdot 10^{-10}$ ,  $1.1 \cdot 10^{-10}$ ,  $1.38 \cdot 10^{-13}$ ,  $2.98 \cdot 10^{-8}$ , 3.35 and  $14.62 \text{ cm}^{-1}$  respectively. The methods used in the study of these molecules, i.e., 1) taking symmetry into account and 2) compiling and solving the vibrational Schrödinger equation of restricted dimensionality, will be applied to analyze the torsional states of the HSSSH molecule as well. Considering that the expected value of the ground vibrational state splitting of the HSSSH trans-conformer should be very small ( $10^{-23} \text{ cm}^{-1}$  [12,13]), the program code for constructing the Hamiltonian matrix and finding its eigenvalues was improved in order to maximize calculation accuracy. This code was also used to refine the tunneling frequencies in the ground and excited torsional states for the first six molecules mentioned above.

## 2. SYMMETRY PROPERTIES

Fig. 1 shows equilibrium configurations of the trans- and cis-conformers of the HSSSH molecule.

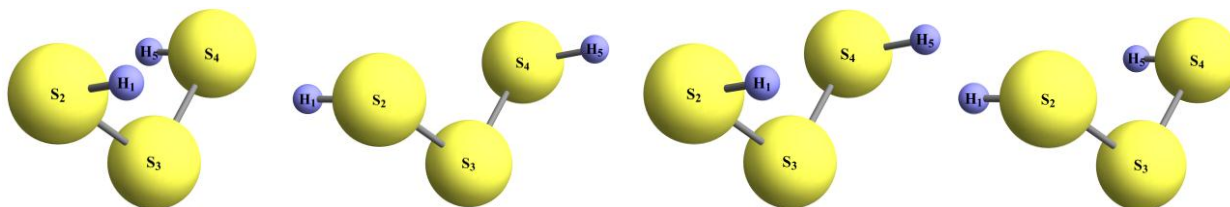


Figure 1. Equilibrium geometries of the trans- (two molecules on the left) and cis- (two molecules on the right) conformers of the HSSSH molecule in two structurally equivalent configurations.

Although the tunneling between equivalent configurations of trans- and cis- conformers of the trisulfane is unlikely, the full 2D potential energy surface formed by rotation the thiol (S-H) groups has  $C_{2v}$  symmetry. Therefore, it is more convenient to classify torsional states of the molecule using the  $C_{2v}(M)$  molecular symmetry group. The elements of this group are the following inversion-permutation symmetry operations: 1) E, 2) (15)(24), 3)  $E^*$ , 4)  $(15)(24)^*$ . The rotations of the  $\text{S}_2\text{-H}_1$  and  $\text{S}_4\text{-H}_5$  groups around the  $\text{S}_3\text{-S}_2$  and  $\text{S}_3\text{-S}_4$  bonds were described using torsional coordinates  $\gamma_1$  and  $\gamma_2$ , respectively. Zero values of these coordinates correspond to the configuration of the molecule shown in Fig.2.

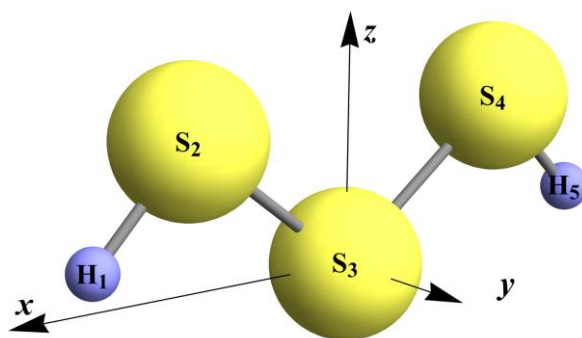


Figure 2. Configuration of the trisulfane molecule, where the values of the two torsional coordinates are considered to be equal to zero. The figure also shows the molecule-fixed Cartesian coordinate system. All atoms lie in the XOZ plane.

As the positive direction of change in the torsional coordinates we chose the clockwise rotation of thiol groups when observing along the  $S_i$ - $S_3$  bonds from the side of the  $S_i$  atom ( $i=2,4$ ). As shown earlier [16-23], potential energy, kinetic coefficients, wave functions, and other physical quantities that are functions of torsional coordinates  $\gamma_1, \gamma_2$  must be either symmetric or antisymmetric with respect to the symmetry elements fixed on the coordinate plane  $\gamma_1, \gamma_2$ , as shown in Fig. 3.

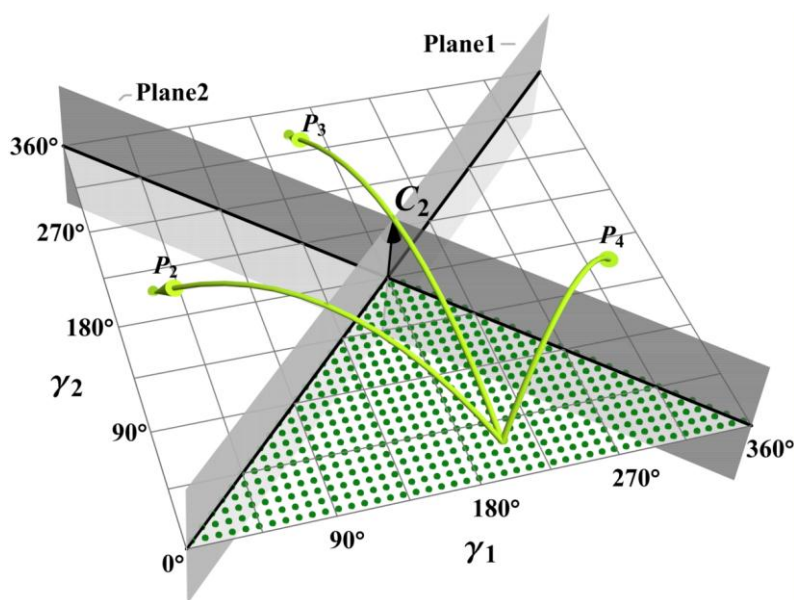


Figure 3. Symmetry elements ( $E$ ,  $C_2$ , Plane 1, Plane 2) of the 2D surfaces of physical quantities functions of torsional coordinates  $\gamma_1, \gamma_2$  of the HSSSH and DSSSD molecules.

Table 1 presents the characters of the irreducible representations of the  $C_{2v}(M)$  molecular symmetry group as well as transformations of the torsional coordinates and some physical quantities under the action of symmetry operations.

Table 1. The characters of the irreducible representations of the  $C_{2v}(M)$  molecular symmetry group. The table indicates by what symmetry species some physical characteristics of the HSSH and DSSSD molecules are transformed, as well as torsional and Cartesian coordinates of the molecule-fixed coordinate system (see Fig. 2).

$C_{2v}(M)$	E	(15)(24)	$E^*$	(15)(24) <sup>*</sup>	
$A_1$	1	1	1	1	$Z, p_z, F_{\gamma_1\gamma_2}, (F_{\gamma_1\gamma_1} + F_{\gamma_2\gamma_2}), U$
$A_2$	1	1	-1	-1	$(\gamma_1, \gamma_2)$
$B_1$	1	-1	1	-1	$X, p_x, (F_{\gamma_1\gamma_1}, F_{\gamma_2\gamma_2})$
$B_2$	1	-1	-1	1	$Y, p_y,$
Transformations of the torsional coordinates	$\gamma_1, \gamma_2$	$\gamma_2, \gamma_1$	$-\gamma_1, -\gamma_2$	$-\gamma_2, -\gamma_1$	
Symmetry elements of the 2D surfaces	E	Reflection in plane 1	Rotation around $C_2$ axis	Reflection in plane 2	
$C_{2v}$	E	$C_2$	$\sigma(XZ)$	$\sigma(YZ)$	

As follows from the data in Table 1, the symmetry requirements lead to the condition (1) for potential energy surface:

$$U(\gamma_1, \gamma_2) = U(\gamma_2, \gamma_1) = U(-\gamma_1, -\gamma_2) = U(-\gamma_2, -\gamma_1); \quad (1)$$

### 3. CALCULATION METHODS

To date, various fruitful approaches to the analysis of large amplitude motions in molecules have been developed [26-36]. In this work, we mainly based on methods, presented in [29,34] and in our previously published works. Molecular characteristics of the trisulfane were calculated at the nodes of an equidistant 2D grid with fixed values of two torsion coordinates using the Gaussian 09 [37] quantum chemical package. First, the calculation was performed at the MP2/Aug-cc-pVTZ level of theory [38-42], and the remaining 3N-8 natural coordinates were optimized, which made it possible to subsequently determine the dependence of the internal energy, kinetic parameters and dipole moment components on the torsional coordinates. Then, geometric parameters that are optimized at each node at the MP2/Aug-cc-pVTZ level of theory were used to calculate the internal energy and dipole moment components at the B3LYP/Aug-cc-pVTZ [43-45], MP2/cc-pVTZ [46], MP2/cc-pVQZ [47,48], and CCSD(T)/Aug-cc-pVTZ [49,50] levels of theory without any optimization of geometric parameters in SP mode. Based on the results obtained on MP2/cc-pVTZ and MP2/cc-pVQZ levels of theory and using known formulas [51,52], the values of the potential energies were extrapolated to the complete basis set (CBS) limit (MP2/CBS(T,Q)). The values of the torsional coordinates were varied in the range from  $4^0$  to  $356^0$  with a step of  $8^0$ . Thus, the calculations were performed at  $45 \times 45 = 2025$  points. After that, the values of the calculated physical quantities were averaged at the points corresponding to the symmetry conditions (1).

The vibrational Schrödinger equation of restricted dimensionality for two torsional coordinates  $(\gamma_1, \gamma_2)$  has a following form [19,23,25]:

$$\left[ -F_{\gamma_1\gamma_1}(\gamma_1, \gamma_2) \frac{\partial^2}{\partial \gamma_1^2} - F_{\gamma_2\gamma_2}(\gamma_1, \gamma_2) \frac{\partial^2}{\partial \gamma_2^2} - F_{\gamma_1\gamma_2}(\gamma_1, \gamma_2) \frac{\partial^2}{\partial \gamma_1 \partial \gamma_2} + U(\gamma_1, \gamma_2) \right] \Psi(\gamma_1, \gamma_2) = E \Psi(\gamma_1, \gamma_2); \quad (2)$$

Kinetic coefficients, potential energy, and wave functions are the functions of coordinates  $\gamma_1$  and  $\gamma_2$ . The 2D surface of kinetic coefficients for the torsional coordinates were calculated using Wilson vectors ( $\vec{s}$  - vectors) [53], (equations (3) for the HSSSH molecule, (4) for the DSSSD molecule and (5) for the DSSSH molecule [17,19,22]).

$$\begin{aligned} F_{\gamma_1\gamma_1} &= B_S \left[ \left( \vec{s}_2^{\gamma_1} \right)^2 + \left( \vec{s}_4^{\gamma_1} \right)^2 + \left( \vec{s}_3^{\gamma_1} \right)^2 \right] + B_H \left( \vec{s}_1^{\gamma_1} \right)^2; \\ F_{\gamma_2\gamma_2} &= B_S \left[ \left( \vec{s}_4^{\gamma_2} \right)^2 + \left( \vec{s}_2^{\gamma_2} \right)^2 + \left( \vec{s}_3^{\gamma_2} \right)^2 \right] + B_H \left( \vec{s}_5^{\gamma_2} \right)^2; \\ F_{\gamma_1\gamma_2} &= 2B_S \left[ \left( \vec{s}_2^{\gamma_1} \cdot \vec{s}_2^{\gamma_2} \right) + \left( \vec{s}_4^{\gamma_1} \cdot \vec{s}_4^{\gamma_2} \right) + \left( \vec{s}_3^{\gamma_1} \cdot \vec{s}_3^{\gamma_2} \right) \right]; \end{aligned} \quad (3)$$

$$\begin{aligned} F_{\gamma_1\gamma_1} &= B_S \left[ \left( \vec{s}_2^{\gamma_1} \right)^2 + \left( \vec{s}_4^{\gamma_1} \right)^2 + \left( \vec{s}_3^{\gamma_1} \right)^2 \right] + B_D \left( \vec{s}_1^{\gamma_1} \right)^2; \\ F_{\gamma_2\gamma_2} &= B_S \left[ \left( \vec{s}_4^{\gamma_2} \right)^2 + \left( \vec{s}_2^{\gamma_2} \right)^2 + \left( \vec{s}_3^{\gamma_2} \right)^2 \right] + B_D \left( \vec{s}_5^{\gamma_2} \right)^2; \\ F_{\gamma_1\gamma_2} &= 2B_S \left[ \left( \vec{s}_2^{\gamma_1} \cdot \vec{s}_2^{\gamma_2} \right) + \left( \vec{s}_4^{\gamma_1} \cdot \vec{s}_4^{\gamma_2} \right) + \left( \vec{s}_3^{\gamma_1} \cdot \vec{s}_3^{\gamma_2} \right) \right]; \end{aligned} \quad (4)$$

$$\begin{aligned} F_{\gamma_1\gamma_1} &= B_S \left[ \left( \vec{s}_2^{\gamma_1} \right)^2 + \left( \vec{s}_4^{\gamma_1} \right)^2 + \left( \vec{s}_3^{\gamma_1} \right)^2 \right] + B_D \left( \vec{s}_1^{\gamma_1} \right)^2; \\ F_{\gamma_2\gamma_2} &= B_S \left[ \left( \vec{s}_4^{\gamma_2} \right)^2 + \left( \vec{s}_2^{\gamma_2} \right)^2 + \left( \vec{s}_3^{\gamma_2} \right)^2 \right] + B_H \left( \vec{s}_5^{\gamma_2} \right)^2; \\ F_{\gamma_1\gamma_2} &= 2B_S \left[ \left( \vec{s}_2^{\gamma_1} \cdot \vec{s}_2^{\gamma_2} \right) + \left( \vec{s}_4^{\gamma_1} \cdot \vec{s}_4^{\gamma_2} \right) + \left( \vec{s}_3^{\gamma_1} \cdot \vec{s}_3^{\gamma_2} \right) \right]; \end{aligned} \quad (5)$$

Here,  $\vec{s}_N^x$  is the Wilson vector corresponding to the coordinate  $x = \{\gamma_1, \gamma_2\}$  and to the atom number  $N$  (numeration of atoms as shown to Fig. 3),  $B_X = \frac{\hbar^2}{2M_X l_0^2}$ ;  $X \in \{H, D, S\}$ ,  $\hbar$  is the Planck's constant,  $l_0 = 1 \text{ \AA}$ ;  $M_H, M_D, M_S$  are the corresponding masses of the hydrogen, deuterium and sulfur atoms.

Equation (2) was solved numerically using the Fourier [54,55] method. Hamiltonian matrix was calculated using the equation:

$$H_{(m,n)(m',n')} = -m^2 F_{m-m',n-n'}^{\gamma_1\gamma_1} - n^2 F_{m-m',n-n'}^{\gamma_2\gamma_2} - mn F_{m-m',n-n'}^{\gamma_1\gamma_2} + U_{m-m',n-n'} \quad (6)$$

where  $F_{m,n}^{\gamma_1\gamma_1}, F_{m,n}^{\gamma_2\gamma_2}, F_{m,n}^{\gamma_1\gamma_2}, U_{m,n}$  were found by fitting coefficients in the equation (2) and employing 2D complex Fourier series (7) using the Mathematica package [56]:

$$\begin{aligned}
F_{\gamma_1\gamma_1}(\gamma_1, \gamma_2) &= \sum_{m,n=-M}^M F_{m,n}^{\gamma_1\gamma_1} e^{i(m\gamma_1+n\gamma_2)}, & F_{\gamma_2\gamma_2}(\gamma_1, \gamma_2) &= \sum_{m,n=-M}^M F_{m,n}^{\gamma_2\gamma_2} e^{i(m\gamma_1+n\gamma_2)}, \\
F_{\gamma_1\gamma_2}(\gamma_1, \gamma_2) &= \sum_{m,n=-M}^M F_{m,n}^{\gamma_1\gamma_2} e^{i(m\gamma_1+n\gamma_2)}, & U(\gamma_1, \gamma_2) &= \sum_{m,n=-M}^M U_{m,n} e^{i(m\gamma_1+n\gamma_2)}
\end{aligned} \tag{7}$$

The wave function is described by a complex two-dimensional Fourier series of the form [54]:

$$\Psi(\gamma_1, \gamma_2) = \sum_{m,n=-N}^N \Psi_{m,n} e^{i(m\gamma_1+n\gamma_2)}, \quad N \succ M; \tag{8}$$

Previously used program code for compiling and diagonalizing the Hamiltonian matrix, implemented in the framework of package [56], was reset to the precision of 32 significant digits for every value of the terms used in calculations. After every numerical operation the preciosity of the output terms was under control. As result of this the preciosity of the calculated eigenvalues and eigenvectors was not worse than 32 significant digits after diagonalization of the Hamiltonian matrix. Herewith, the time required to diagonalize the Hamiltonian matrix increases by several orders of magnitude.

The intensities of the torsional transitions were calculated using equation (9) [57-62]:

$$I_{i \rightarrow f} = \frac{Const \cdot \tilde{\nu}_{if} \cdot \left( e^{-\frac{E_i - E_l}{kT}} - e^{-\frac{E_f - E_l}{kT}} \right)}{Q(T)} p_{if}^2; \quad Q(T) = \sum_i e^{-\frac{E_i - E_l}{kT}}; \tag{9}$$

Here  $Q(T)$  - partition function over torsional states,  $i, f$  - denote initial and final states,  $\tilde{\nu}_{if}$  - wave number for a transition from initial to a final state,  $p_{if}^2$  - square of the matrix element of the dipole moment operator, which was calculated by the equation (10) using the package [56],  $Const$  in equation (9) was set to 0.1.

$$p_{if}^2 = \sum_{k=x,y,z} \left( \int_{\gamma_1=0}^{2\pi} \int_{\gamma_2=0}^{2\pi} \Psi_i(\gamma_1, \gamma_2) p_k(\gamma_1, \gamma_2) \Psi_f(\gamma_1, \gamma_2) d\gamma_1 d\gamma_2 \right)^2 \tag{10}$$

## 4. DISCUSSION OF THE RESULTS OF CALCULATIONS

### 4.1 Barriers to internal rotations and 2D PES parameters of the HO(CH<sub>2</sub>)OH , HOOH, HSOSH, HOSOH and HSSSH molecules.

As noted in the introduction, the new algorithm for compiling and diagonalizing the Hamiltonian matrix was used both for the trisulfane molecule and for five more previously studied molecules in order to refine the values of the stationary torsional states splittings. This also made it possible to compare the relative energies of the trans- and cis- conformers of these molecules, as well as the parameters of potential barriers between the equivalent configurations.



Fig. 4 shows 2D PES of the  $\text{HO}(\text{CH}_2)\text{OH}$ ,  $\text{HOOOH}$ ,  $\text{HSOSH}$ ,  $\text{HOSOH}$  and  $\text{HSSSH}$  molecules with equi-energy contours.

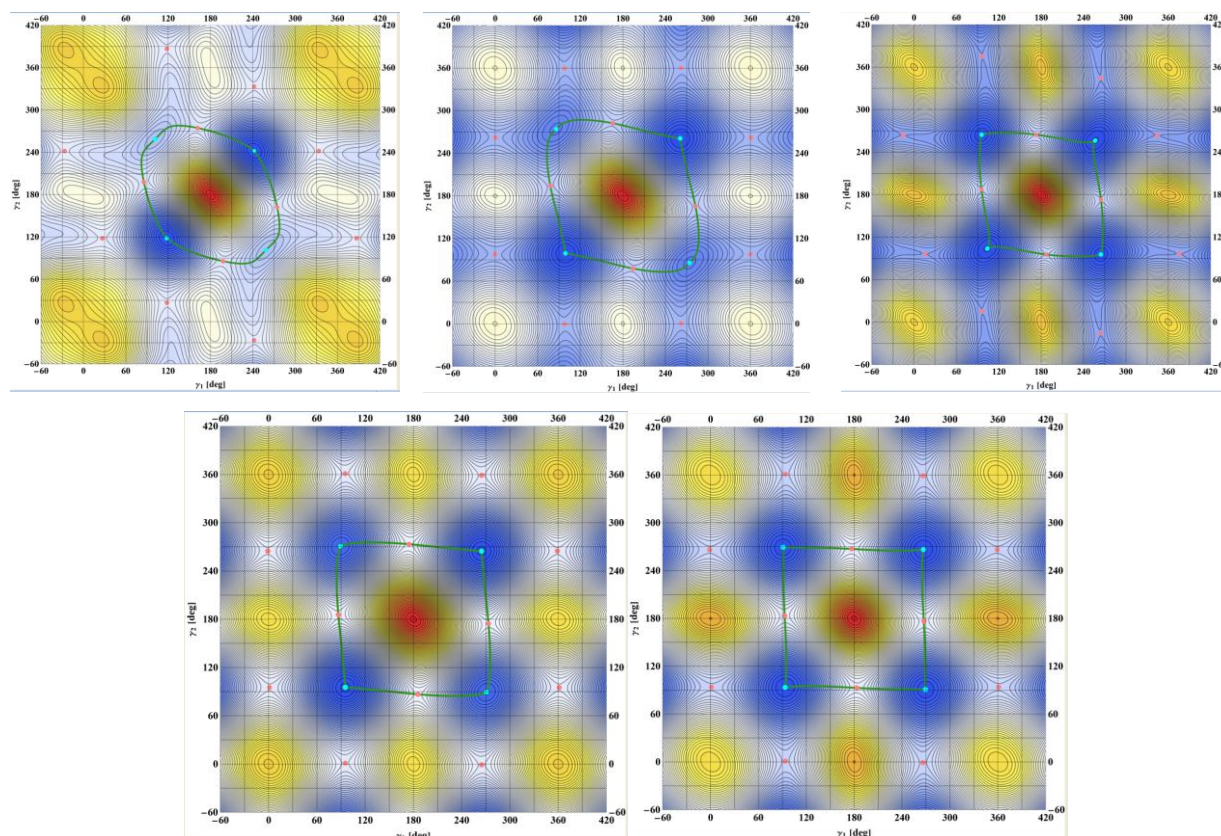


Figure 4. Equi-energy contours of the potential energy surfaces of molecules:  $\text{HO}(\text{CH}_2)\text{OH}$  (left, top row),  $\text{HOOOH}$  (center, top row),  $\text{HSOSH}$  (right, top row),  $\text{HOSOH}$  (left, bottom row) and  $\text{HSSSH}$  (right, bottom row). Saturated blue color corresponds to a decrease in energy, and saturated yellow and red colors correspond to an increase in energy. Green curves show the minimum energy paths of transitions between the equilibrium configurations of molecular conformers.

Fig.5 makes it possible to quantify the difference in the potential barriers when moving along the green curves in Fig.4 which characterize the minimum energy paths during the movement from the global minimum (trans- conformer) to the local one (cis- conformer), then to the equivalent global and local minima, and finally to the initial global minimum.



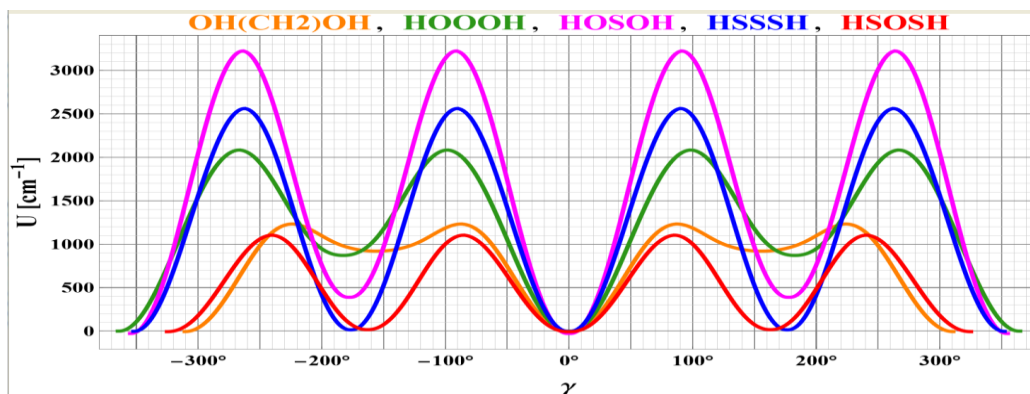


Figure 5. Comparison of the potential barriers arising when moving along the green curves in Fig. 4 for molecules: HO(CH<sub>2</sub>)OH - orange, HOOOH – green, HSOSH - red, HOSOH – pink, and HSSSH – blue.

As follows from Fig. 5, all five studied molecules are characterized by approximately the same location of the local and global minima on the 2D PES. Relative energy of the cis-conformers decreases in the following order: HOOOH, HO(CH<sub>2</sub>)OH, HOSOH, HSOSH, HSSSH, whereas the height of the potential barriers increases in the following order: HSOSH, HO(CH<sub>2</sub>)OH, HOOOH, HSSSH, HOSOH.

#### 4.2 Results of the variational vibrational calculations.

Consider next the update results of calculations of the ground vibrational state tunneling splittings of the five analyzed molecules. The values of the tunneling frequencies in the ground vibrational state calculated in this work for the trans- and cis- conformers of the HO(CH<sub>2</sub>)OH, HOOOH, HSOSH, HOSOH, HSSSH and C<sub>6</sub>H<sub>4</sub>(OH)<sub>2</sub> molecules and some of their deuterated analogs are presented in Table 2.

Table 2. Calculated values of the tunneling frequencies in the ground vibrational state in molecules HO(CH<sub>2</sub>)OH, HOOOH, HSOSH, HOSOH, HSSSH and C<sub>6</sub>H<sub>4</sub>(OH)<sub>2</sub>-ortho.

Molecule	HO(CH <sub>2</sub> )OH		C <sub>6</sub> H <sub>4</sub> (OH) <sub>2</sub> -ortho		HOOOH	
Conformer	Trans	Cis	C <sub>s</sub>	C <sub>2v</sub>	Trans	Cis
Tunneling frequency [cm <sup>-1</sup> ]	2.4*10 <sup>-6</sup>	3.3*10 <sup>-1</sup>	3.0*10 <sup>-8</sup>	-	1,3*10 <sup>-11</sup>	2.9*10 <sup>-7</sup>
Molecule	HSOSH		HOSOH		HSSSH	
Conformer	Trans	Cis	Trans	Cis	Trans	Cis
Tunneling frequency [cm <sup>-1</sup> ]	2.3*10 <sup>-11</sup>	3.7*10 <sup>-11</sup>	1.3*10 <sup>-15</sup>	5.0*10 <sup>-16</sup>	2.2*10 <sup>-20</sup>	2.4*10 <sup>-21</sup>
Molecule	DO(CH <sub>2</sub> )OD		C <sub>6</sub> H <sub>4</sub> (OD) <sub>2</sub> -ortho		DOOOD	
Conformer	Trans	Cis	C <sub>s</sub>	C <sub>2v</sub>	Trans	Cis
Tunneling frequency [cm <sup>-1</sup> ]	1.8*10 <sup>-9</sup>	1.4*10 <sup>-2</sup>	-	-	3.2*10 <sup>-16</sup>	2.3*10 <sup>-10</sup>
Molecule	DSOSD		DOSOD		DSSSD	
Conformer	Trans	Cis	Trans	Cis	Trans	Cis
Tunneling frequency [cm <sup>-1</sup> ]	3.2*10 <sup>-16</sup>	2.1*10 <sup>-16</sup>	2.4*10 <sup>-19</sup>	2.8*10 <sup>-16</sup>	7.5*10 <sup>-27</sup>	1.1*10 <sup>-28</sup>

As follows from the data in Table 2, the tunneling frequencies for six molecules differ by more than ten orders of magnitude. For the  $\text{HO}(\text{CH}_2)\text{OH}$  and  $\text{C}_6\text{H}_4(\text{OH})_{2\text{-ortho}}$  molecules, the tunneling frequencies in the ground vibrational state calculated in this work and in previous works [16,23] using simpler and faster algorithms, completely align. In the case of  $\text{HOOOH}$  and  $\text{HSOSH}$  molecules, the tunneling frequencies in the ground vibrational state calculated in this work using a more advanced but much more time-consuming algorithm, turned out to be an order of magnitude lower than the values obtained earlier in [19] and [20]. As for the  $\text{HOSOH}$  molecule, the tunneling frequency calculated in this work turned out to be two orders of magnitude lower than the value obtained in [22]. Also, according to the data of Table 2, the tunneling frequencies obtained in this work for deuterated molecules turned out to be 2-5 orders of magnitude lower than in the simpler algorithm case. As follows from the data in Table 2, the maximum tunneling frequency for trans- conformers is realized in the  $\text{HO}(\text{CH}_2)\text{OH}$  molecule ( $2.4 \cdot 10^{-6} \text{ cm}^{-1}$ ), and the minimum frequency ( $2.2 \cdot 10^{-20} \text{ cm}^{-1}$ ) is in the trisulfane molecule. The latter value appeared to be quite close to the estimation made in [12,13] ( $10^{-23} \text{ cm}^{-1}$ ). It is clear that if a) the tunneling frequency in the trans- conformer of the trisulfane molecule turns out to be in the range of  $10^{-20} - 10^{-23} \text{ cm}^{-1}$  and b) the splittings of the energy levels due to the violation of parity law in the analyzed molecule will be really of the order of  $10^{-12} \text{ cm}^{-1}$ , as estimated by the authors of [12,13], then a) will not interfere with the experimental observation of b) in the  $\text{HSSSH}$  molecule.

Although the potential barriers to internal rotation are more than  $500 \text{ cm}^{-1}$  higher in  $\text{HOSOH}$  than in  $\text{HSSSH}$  (see Fig.5), the tunneling frequency in the latter is 5 orders of magnitude lower. This is due to the kinetic parameters in the  $\text{HSSSH}$  molecule being two times smaller than in the  $\text{HOSOH}$  molecule, which is happening because of the difference in geometric parameters of the thiol and hydroxyl groups. Calculated at the  $\text{CCSD(T)}/\text{Aug-cc-pVTZ}$  level of theory Figures of the 2D surfaces of the kinetic parameters, dipole moment components, potential barriers with stationary torsional levels of the trans- and cis- conformers, and potential energy of the  $\text{HSSSH}$  molecule are given in Supplementary Materials Part I.

Table 3 shows the energies of the stationary torsional states of the  $\text{HSSSH}$  molecule calculated at the  $\text{B3LYP}/\text{Aug-cc-pVTZ}$ ,  $\text{MP2}/\text{Aug-cc-pVTZ}$ , and  $\text{CCSD(T)}/\text{Aug-cc-pVTZ}$  levels of theory. Table 4 shows the energies of the stationary torsional states of the  $\text{HSSSH}$  molecule calculated at the  $\text{MP2}/\text{cc-pVTZ}$ ,  $\text{MP2}/\text{Aug-cc-pVTZ}$ ,  $\text{MP2}/\text{cc-pVQZ}$ , and  $\text{MP2}/\text{CBS(T,Q)}$  levels of theory.

**Table 3.** The values of a) the energies of stationary torsional states, b) torsional quantum numbers, c) symmetry species in the molecular symmetry group  $\text{C}_{2v}(\text{M})$ , and the description of

the conformational states of the HSSSH molecule, calculated at the B3LYP/Aug-cc-pVTZ, MP2/Aug-cc-pVTZ, and CCSD(T) /Aug-cc-pVTZ levels of theory.

Symmetry species	Conformation	$n_{as}$	$n_s$	B3LYP/Aug-cc-pVTZ		MP2/Aug-cc-pVTZ		CCSD(T)/Aug-cc-pVTZ	
				Energy [cm <sup>-1</sup> ]	Energy splitting [cm <sup>-1</sup> ]	Energy [cm <sup>-1</sup> ]	Energy splitting [cm <sup>-1</sup> ]	Energy [cm <sup>-1</sup> ]	Energy splitting [cm <sup>-1</sup> ]
A <sub>1</sub> +A <sub>2</sub>	trans	0	0	0	7.70*10 <sup>-19</sup>	0	1.28*10 <sup>-20</sup>	0	2.19*10 <sup>-20</sup>
A <sub>1</sub> -A <sub>2</sub>	trans	0	0	7.70*10 <sup>-19</sup>		1.28*10 <sup>-20</sup>		2.19*10 <sup>-20</sup>	
B <sub>2</sub>	cis	0	0	25.125	2.96*10 <sup>-22</sup>	18.510	1.27*10 <sup>-21</sup>	23.018	2.36*10 <sup>-21</sup>
A <sub>1</sub>	cis	0	0	25.125		18.510		23.018	
A <sub>2</sub>	trans	0	1	305.452	1.79*10 <sup>-17</sup>	297.386	5.81*10 <sup>-18</sup>	293.575	5.63*10 <sup>-18</sup>
A <sub>1</sub>	trans	0	1	305.452		297.386		293.575	
B <sub>2</sub>	trans	1	0	325.103	2.31*10 <sup>-17</sup>	323.555	1.48*10 <sup>-17</sup>	317.616	1.82*10 <sup>-17</sup>
B <sub>1</sub>	trans	1	0	325.103		323.555		317.616	
A <sub>2</sub>	cis	1	0	340.432	1.02*10 <sup>-18</sup>	329.641	1.55*10 <sup>-17</sup>	327.102	5.23*10 <sup>-18</sup>
B <sub>1</sub>	cis	1	0	340.432		329.641		327.102	
A <sub>1</sub>	cis	0	1	351.296	4.27*10 <sup>-19</sup>	343.207	3.45*10 <sup>-16</sup>	341.362	4.47*10 <sup>-16</sup>
B <sub>2</sub>	cis	0	1	351.296		343.207		341.362	
A <sub>1</sub>	trans	0	2	605.221	1.29*10 <sup>-16</sup>	589.243	1.58*10 <sup>-15</sup>	581.526	2.85*10 <sup>-15</sup>
A <sub>2</sub>	trans	0	2	605.221		589.243		581.526	
B <sub>1</sub>	trans	1	1	616.364	1.00*10 <sup>-16</sup>	606.261	2.55*10 <sup>-14</sup>	596.864	5.33*10 <sup>-14</sup>
B <sub>2</sub>	trans	1	1	616.364		606.261		596.864	
B <sub>2</sub>	cis	2	0	647.131	7.11*10 <sup>-14</sup>	632.196	7.87*10 <sup>-14</sup>	623.137	1.94*10 <sup>-12</sup>
A <sub>1</sub>	cis	2	0	647.131		632.196		623.137	
A <sub>2</sub>	cis	1	1	647.493	7.61*10 <sup>-14</sup>	639.888	5.60*10 <sup>-14</sup>	631.283	1.89*10 <sup>-12</sup>
B <sub>1</sub>	cis	1	1	647.493		639.888		631.283	
A <sub>1</sub>	trans	2	0	652.487	5.24*10 <sup>-15</sup>	643.287	1.48*10 <sup>-15</sup>	631.517	2.08*10 <sup>-15</sup>
A <sub>2</sub>	trans	2	0	652.487		643.287		631.517	
B <sub>2</sub>	cis	0	2	675.470	1.01*10 <sup>-15</sup>	665.218	3.11*10 <sup>-14</sup>	656.934	6.15*10 <sup>-14</sup>
A <sub>1</sub>	cis	0	2	675.470		665.218		656.934	
A <sub>2</sub>	trans	0	3	896.575	1.09*10 <sup>-14</sup>	873.543	1.11*10 <sup>-13</sup>	861.835	2.04*10 <sup>-13</sup>
A <sub>1</sub>	trans	0	3	896.575		873.543		861.835	
B <sub>1</sub>	trans	1	2	900.001	1.63*10 <sup>-13</sup>	881.366	7.30*10 <sup>-12</sup>	868.526	1.23*10 <sup>-11</sup>
B <sub>2</sub>	trans	1	2	900.001		881.366		868.526	
A <sub>2</sub>	trans	2	1	928.646	4.51*10 <sup>-13</sup>	914.425	4.93*10 <sup>-11</sup>	899.746	7.62*10 <sup>-11</sup>
A <sub>1</sub>	trans	2	1	928.646		914.425		899.746	

**Table 4.** The values of a) the energies of stationary torsional states, b) torsional quantum numbers, c) symmetry species in the molecular symmetry group C<sub>2v</sub>(M), and the description of the conformational states of the HSSSH molecule, calculated at the MP2/cc-pVTZ, MP2/Aug-cc-pVTZ, MP2/cc-pVQZ, and MP2 /CBS(T,Q) levels of theory.

Symmetry species	Conformation	$n_{as}$	$n_s$	MP2/cc-pVTZ		MP2/Aug-cc-pVTZ		MP2/cc-pVQZ		MP2/CBS(T,Q)	
				Energy [cm <sup>-1</sup> ]	Energy splitting [cm <sup>-1</sup> ]	Energy [cm <sup>-1</sup> ]	Energy splitting [cm <sup>-1</sup> ]	Energy [cm <sup>-1</sup> ]	Energy splitting [cm <sup>-1</sup> ]	Energy [cm <sup>-1</sup> ]	Energy splitting [cm <sup>-1</sup> ]
A <sub>1</sub> +A <sub>2</sub>	trans	0	0	0	8.03*10 <sup>-20</sup>	0	1.28*10 <sup>-20</sup>	0	4.24*10 <sup>-20</sup>	0	1.01*10 <sup>-20</sup>
A <sub>1</sub> -A <sub>2</sub>	trans	0	0	8.03*10 <sup>-20</sup>		1.28*10 <sup>-20</sup>		4.24*10 <sup>-20</sup>		1.01*10 <sup>-20</sup>	
B <sub>2</sub>	cis	0	0	44.386	4.38*10 <sup>-22</sup>	18.510	1.27*10 <sup>-21</sup>	24.417	4.83*10 <sup>-22</sup>	21.022	8.36*10 <sup>-22</sup>
A <sub>1</sub>	cis	0	0	44.386		18.510		24.417		21.022	
A <sub>2</sub>	trans	0	1	301.167	7.21*10 <sup>-18</sup>	297.386	5.81*10 <sup>-18</sup>	299.008	5.85*10 <sup>-18</sup>	295.427	4.91*10 <sup>-18</sup>
A <sub>1</sub>	trans	0	1	301.167		297.386		299.008		295.427	
B <sub>2</sub>	trans	1	0	327.187	8.22*10 <sup>-18</sup>	323.555	1.48*10 <sup>-17</sup>	322.732	3.87*10 <sup>-18</sup>	316.129	1.93*10 <sup>-17</sup>
B <sub>1</sub>	trans	1	0	327.187		323.555		322.732		316.129	
A <sub>2</sub>	cis	1	0	355.262	1.50*10 <sup>-18</sup>	329.641	1.55*10 <sup>-17</sup>	340.769	3.11*10 <sup>-18</sup>	325.321	1.04*10 <sup>-17</sup>
B <sub>1</sub>	cis	1	0	355.262		329.641		340.769		325.321	
A <sub>1</sub>	cis	0	1	372.281	7.15*10 <sup>-18</sup>	343.207	3.45*10 <sup>-16</sup>	353.359	7.17*10 <sup>-17</sup>	339.749	2.74*10 <sup>-17</sup>
B <sub>2</sub>	cis	0	1	372.281		343.207		353.359		339.749	
A <sub>1</sub>	trans	0	2	596.328	7.24*10 <sup>-17</sup>	589.243	1.58*10 <sup>-15</sup>	591.037	5.37*10 <sup>-16</sup>	584.859	9.27*10 <sup>-16</sup>
A <sub>2</sub>	trans	0	2	596.328		589.243		591.037		584.859	
B <sub>1</sub>	trans	1	1	613.552	3.55*10 <sup>-16</sup>	606.261	2.55*10 <sup>-14</sup>	608.769	2.58*10 <sup>-15</sup>	599.462	5.99*10 <sup>-15</sup>
B <sub>2</sub>	trans	1	1	613.552		606.261		608.769		599.462	
B <sub>2</sub>	cis	2	0	650.576	7.27*10 <sup>-15</sup>	632.196	7.87*10 <sup>-14</sup>	639.263	2.15*10 <sup>-14</sup>	628.147	6.32*10 <sup>-14</sup>
A <sub>1</sub>	cis	2	0	650.576		632.196		639.263		628.147	
A <sub>2</sub>	cis	1	1	657.924	1.19*10 <sup>-14</sup>	639.888	5.60*10 <sup>-14</sup>	644.786	2.61*10 <sup>-14</sup>	635.308	3.98*10 <sup>-14</sup>
B <sub>1</sub>	cis	1	1	657.924		639.888		644.786		635.308	
A <sub>1</sub>	trans	2	0	668.314	5.22*10 <sup>-15</sup>	643.287	1.48*10 <sup>-15</sup>	650.930	3.54*10 <sup>-14</sup>	636.673	7.92*10 <sup>-14</sup>
A <sub>2</sub>	trans	2	0	668.314		643.287		650.930		636.673	
B <sub>2</sub>	cis	0	2	697.183	3.37*10 <sup>-16</sup>	665.218	3.11*10 <sup>-14</sup>	672.786	4.78*10 <sup>-15</sup>	661.455	7.79*10 <sup>-15</sup>
A <sub>1</sub>	cis	0	2	697.183		665.218		672.786		661.455	
A <sub>2</sub>	trans	0	3	883.609	1.50*10 <sup>-14</sup>	873.543	1.11*10 <sup>-13</sup>	875.881	1.44*10 <sup>-14</sup>	868.821	1.12*10 <sup>-14</sup>
A <sub>1</sub>	trans	0	3	883.609		873.543		875.881		868.821	
B <sub>1</sub>	trans	1	2	891.877	4.52*10 <sup>-14</sup>	881.366	7.30*10 <sup>-12</sup>	880.754	3.97*10 <sup>-13</sup>	873.697	8.89*10 <sup>-13</sup>
B <sub>2</sub>	trans	1	2	891.877		881.366		880.754		873.697	
A <sub>2</sub>	trans	2	1	925.127	5.36*10 <sup>-13</sup>	914.425	4.93*10 <sup>-11</sup>	915.348	6.22*10 <sup>-12</sup>	906.837	1.16*10 <sup>-11</sup>
A <sub>1</sub>	trans	2	1	925.127		914.425		915.348		906.837	

The energies of stationary torsional states of the DSSSH and DSSSD molecules calculated at the CCSD(T)/Aug-cc-pVTZ level of theory can be found in Table 5.

**Table 5.** Calculated at the CCSD(T)/Aug-cc-pVTZ level of theory a) energies of stationary torsional states, b) torsional quantum numbers, c) symmetry species in the molecular symmetry groups  $C_s(M)$  and  $C_{2v}(M)$ , and the types of the conformations of the DSSSH and DSSSD molecules.

1	2	3	4	5	6	7	8	9	10	11	12	13
DSSSD							HSSSD					
Energy level number N	Conformation	Energy [cm <sup>-1</sup> ]	Energy splitting [cm <sup>-1</sup> ]	$n_{as}$	$n_s$	Symmetry species	Conformation	Energy [cm <sup>-1</sup> ]	Energy splitting [cm <sup>-1</sup> ]	$n_{SH}$	$n_{SD}$	Symmetry species
1	trans	0	7.48*10 <sup>-27</sup>	0	0	A <sub>1</sub> +A <sub>2</sub>	trans	0	2.29*10 <sup>-25</sup>	0	0	A'
2	trans	7.48*10 <sup>-27</sup>		0	0	A <sub>1</sub> -A <sub>2</sub>	trans	2.29*10 <sup>-25</sup>		0	0	A''
3	cis	21.35	1.06*10 <sup>-28</sup>	0	0	A <sub>1</sub>	cis	22.19	1.11*10 <sup>-25</sup>	0	0	A'
4	cis	21.35		0	0	B <sub>2</sub>	cis	22.19		0	0	A''
5	trans	214.05	1.65*10 <sup>-25</sup>	0	1	A <sub>1</sub>	trans	224.98	5.28*10 <sup>-24</sup>	0	1	A'
6	trans	214.05		0	1	A <sub>2</sub>	trans	224.98		0	1	A''
7	trans	237.92	6.48*10 <sup>-27</sup>	1	0	B <sub>1</sub>	cis	251.81	6.05*10 <sup>-24</sup>	0	1	A'
8	trans	237.92		1	0	B <sub>2</sub>	cis	251.81		0	1	A''
9	cis	243.47	4.14*10 <sup>-26</sup>	1	0	B <sub>1</sub>	trans	306.95	3.32*10 <sup>-23</sup>	1	0	A'
10	cis	243.47		1	0	A <sub>2</sub>	trans	306.95		1	0	A''
11	cis	259.44	5.96*10 <sup>-27</sup>	0	1	B <sub>2</sub>	cis	333.83	1.14*10 <sup>-23</sup>	1	0	A'
12	cis	259.44		0	1	A <sub>1</sub>	cis	333.83		1	0	A''
13	trans	425.49	2.23*10 <sup>-24</sup>	0	2	A <sub>1</sub>	trans	442.56	1.52*10 <sup>-22</sup>	0	2	A'
14	trans	425.49		0	2	A <sub>2</sub>	trans	442.56		0	2	A''
15	trans	444.44	2.69*10 <sup>-24</sup>	1	1	B <sub>2</sub>	cis	474.52	4.52*10 <sup>-22</sup>	0	2	A'
16	trans	444.44		1	1	B <sub>1</sub>	cis	474.52		0	2	A''
17	cis	462.01	2.02*10 <sup>-23</sup>	2	0	B <sub>2</sub>	trans	532.23	1.05*10 <sup>-21</sup>	1	1	A'
18	cis	462.01		2	0	A <sub>1</sub>	trans	532.23		1	1	A''
19	trans	473.51	3.29*10 <sup>-22</sup>	2	0	A <sub>1</sub>	cis	564.18	4.24*10 <sup>-21</sup>	1	1	A'
20	trans	473.51		2	0	A <sub>2</sub>	cis	564.18		1	1	A''
21	cis	474.11	8.14*10 <sup>-22</sup>	1	1	B <sub>1</sub>	trans	601.46	7.09*10 <sup>-21</sup>	2	0	A'
22	cis	474.11		1	1	A <sub>2</sub>	trans	601.46		2	0	A''
23	cis	495.54	1.77*10 <sup>-24</sup>	0	2	B <sub>2</sub>	cis	632.56	9.21*10 <sup>-21</sup>	2	0	A'
24	cis	495.54		0	2	A <sub>1</sub>	cis	632.56		2	0	A''
25	trans	634.03	7.68*10 <sup>-23</sup>	0	3	A <sub>2</sub>	trans	653.71	3.58*10 <sup>-21</sup>	0	3	A'
26	trans	634.03		0	3	A <sub>1</sub>	trans	653.71		0	3	A''
27	trans	647.70	8.36*10 <sup>-22</sup>	1	2	B <sub>1</sub>	cis	689.85	2.13*10 <sup>-20</sup>	0	3	A'
28	trans	647.70		1	2	B <sub>2</sub>	cis	689.85		0	3	A''
29	trans	673.10	8.11*10 <sup>-20</sup>	2	1	A <sub>2</sub>	trans	751.38	6.93*10 <sup>-20</sup>	1	2	A'
30	trans	673.10		2	1	A <sub>1</sub>	trans	751.38		1	2	A''

As can be seen from Tables 3 and 4, the ground torsional state of cis-conformer of HSSSH is only 20 cm<sup>-1</sup> higher than the one of the trans-conformer. In the DSSSD molecule, energy difference between the ground states of cis- and trans-conformers is 21.4 cm<sup>-1</sup>. These values are close to the corresponding values of HSOSH and DSOSD [20], and the reasons for such similar energies are described in [20]. It also follows from Tables 3,4 and 5 that the tunneling frequencies in the excited torsional states of the HSSSH and DSSSD molecules turn out to be very low. Table 3 gives us the possibility to compare B3LYP, MP2 and CCSD(T) levels of theory in application to 2D PES calculations of the HSSSH molecule. All three levels used the same Aug-cc-pVTZ basis set. One can see for all levels very close results in determination of the values of the tunneling splittings. However, values of the torsional levels differ significantly. This is more obvious for B3LYP from one hand and MP2, CCSD(T) from other hand. Of course we sure the most exact result obtained at CCSD(T) level of theory. Tabl.4 lets us compare the dependence of the calculated 2D PES of the HSSSH molecule on the completeness of the basis set used. One can see the values of tunneling splittings for all basis sets used are close, however

values of the torsional levels differ again. It should be noted that the results calculated at the CCSD(T)/Aug-cc-pVTZ and MP2/CBS(T,Q) levels of theory are most close.

### 4.3 Comparison of the harmonic, anharmonic and variational results of calculations of the S-H torsional vibration frequencies.

Torsional vibrations of the trisulfane molecule were also calculated in the harmonic and anharmonic approximations at the MP2/Aug-cc-pVTZ level of theory. It is important to note that according to the data of the anharmonic calculations torsional vibrational modes and their overtones do not take part in Fermi or Darling-Dannison types of resonances. This serves as an additional argument in favor of the validity of considering the torsion vibrations of both conformers of the molecule as a separate vibrational problem of restricted dimensionality. In Tabl.6 there were gathering results of the harmonic, anharmonic and variational calculations of the frequencies of the fundamental and overtones of the torsional vibrations of the trans- and cis-conformers of the HSSSH molecule.

Table 6 Frequencies of the fundamental, overtones and combinations of the torsional vibrations of the trans- and cis- HSSSH conformers calculated at different approximations.

Level of theory	$\tilde{\nu}_s$ [cm <sup>-1</sup> ]	$\tilde{\nu}_{as}$ [cm <sup>-1</sup> ]	$2\tilde{\nu}_s$ [cm <sup>-1</sup> ]	$2\tilde{\nu}_{as}$ [cm <sup>-1</sup> ]	$\tilde{\nu}_s + \tilde{\nu}_{as}$ [cm <sup>-1</sup> ]
Trans-conformer					
MP2/Aug-cc-pVTZ (harm)	309	334	-	-	-
MP2/Aug-cc-pVTZ (anharm)	297	321	590	639	607
CCSD(T)/Aug-cc-pVTZ(2D PES)	294	318	582	632	597
Cis-conformer					
MP2/Aug-cc-pVTZ (harm)	335	323	-	-	-
MP2/Aug-cc-pVTZ (anharm)	321	309	639	613	620
CCSD(T)/Aug-cc-pVTZ(2D PES)	318	304	634	600	608

As follows from the data in Table 6, calculated by solving vibrational Schrödinger equation frequencies of the symmetric and antisymmetric fundamental torsional vibrations in trans- and cis-conformers of the HSSSH molecule turned out to be  $\tilde{\nu}_s^{trans}=294$ ,  $\tilde{\nu}_{as}^{trans}=318$  and  $\tilde{\nu}_s^{cis}=318$ ,  $\tilde{\nu}_{as}^{cis}=304$  cm<sup>-1</sup>, respectively. Since the potential barriers separating the trans- and cis-conformers are quite large, calculated values of these frequencies in the anharmonic approximation (  $\tilde{\nu}_s^{trans}=297$ ,  $\tilde{\nu}_{as}^{trans}=321$  and  $\tilde{\nu}_s^{cis}=321$ ,  $\tilde{\nu}_{as}^{cis}=309$  cm<sup>-1</sup>) appear to be very close to the values, obtained using the numerical solution of the vibrational Schrödinger equation. The calculated in the anharmonic approximation frequencies of the overtones and combinations of the torsional HSSSH vibrations not much so good with data, obtained by variational method, as it was for fundamental vibrations (see Tabl. 6). The harmonic approximation overestimates the

frequencies of torsional vibrations of the HSOSH molecule by  $15\text{ cm}^{-1}$  on average ( $\tilde{\nu}_s^{trans}=309$ ,  $\tilde{\nu}_{as}^{trans}=334$  и  $\tilde{\nu}_s^{cis}=335$ ,  $\tilde{\nu}_{as}^{cis}=323\text{ cm}^{-1}$ ).

#### 4.4 Results of calculations of the torsional IR spectra of the trisulfane molecule.

Fig. 6 presents the torsional IR spectra of trans- and cis-conformers of the HSSSH molecule calculated at the CCSD(T)/Aug-cc-pVTZ level of theory in the absence of rotation (for example, in matrix isolation) at the temperatures of 300 and 30 K.

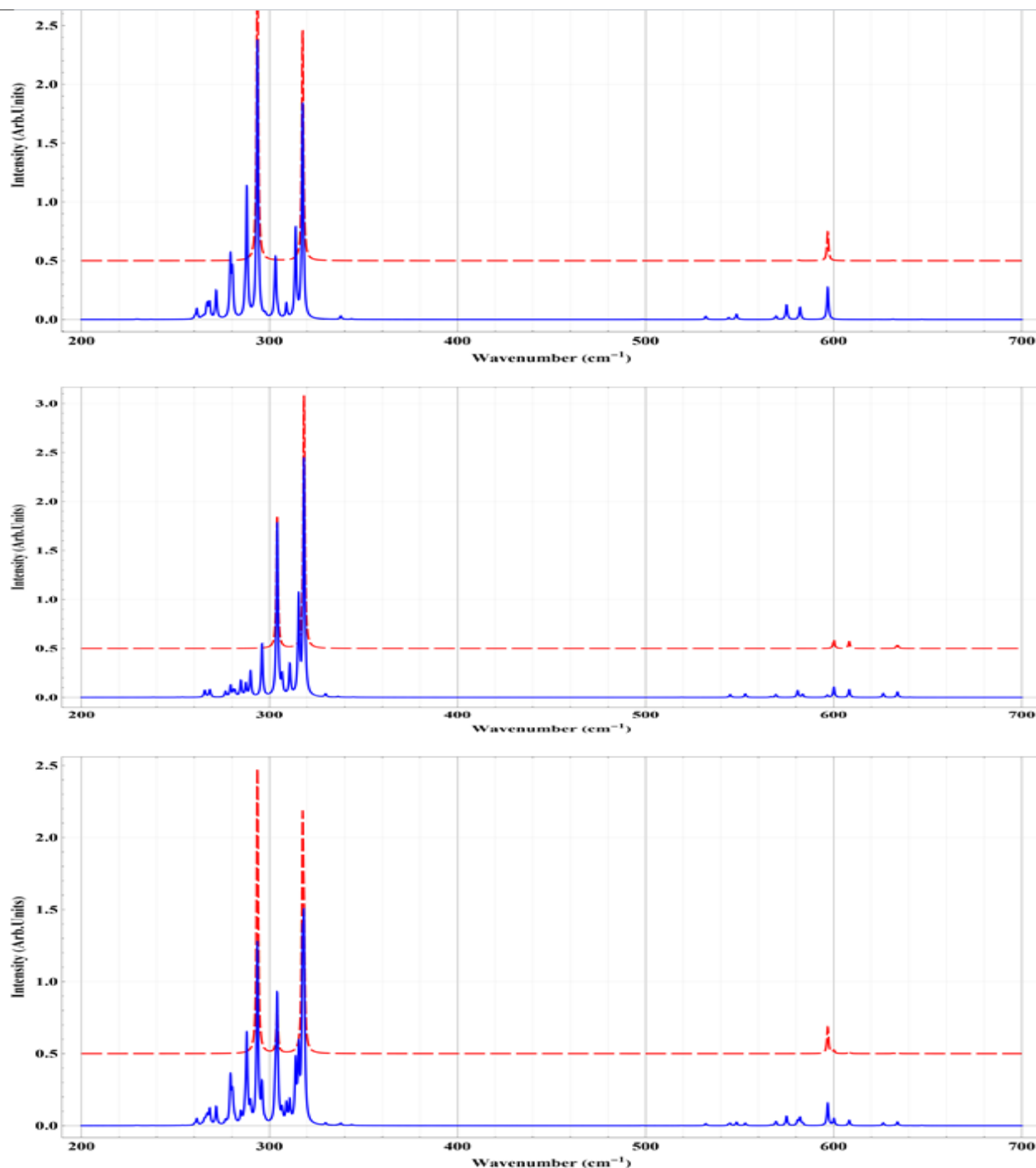


Figure 6. Calculated at the CCSD(T)/Aug-cc-pVTZ level of theory, HSSSH torsional IR spectra of trans- (upper figure) and cis- (middle figure) conformers, as well as the mixture of



conformers in the thermodynamic equilibrium (lower figure) at the temperatures of 300 K (blue color) and 30 K (red).

Similar torsional IR absorption spectra for the trans- and cis-conformers of DSSSH and DSSSD can be found in Supplementary Materials Part I.

As can be seen from Fig.6, calculated IR torsional spectra of the trans- and cis-conformers of the HSSSH molecule are significantly different and contain a fairly large number of absorption bands at  $T=300$  K, most of which are due to transitions from excited torsional states. At a temperature of 30 K, the number of absorption bands decreases as expected. We also note that calculations at all approximations predict that the frequencies of the antisymmetric torsional vibration of thiol groups in the trans-conformer ( $318\text{ cm}^{-1}$ ) and the symmetric torsional vibration in the cis-conformer ( $319\text{ cm}^{-1}$ ) practically match. Therefore, for qualitative and quantitative analysis of the composition consisting of the HSSSH conformers mixture, one should use the symmetric torsional vibration of thiol groups in the trans-conformer which should appear around  $294\text{ cm}^{-1}$ , and the antisymmetric torsional vibration of thiol groups in the cis-conformer which should reveal itself around  $304\text{ cm}^{-1}$  according to calculations. All information about the assignment of absorption bands in the 1) IR spectra of the HSSSH molecule shown in Fig. 6, 2) IR spectra of the DSSSD and DSSSH molecules shown in Fig. 5 and 6 of the Supplementary Materials Part I, is given in Supplementary Materials Part II.

## CONCLUSIONS

In this work, torsional vibrations of molecules HSSSH, DSSSH, and DSSSD are analyzed in the harmonic and anharmonic approximations, as well as by constructing 2D PES defined by the rotation of thiol groups and calculated at several levels of theory. It has been established that the energies of trans- and cis-conformers are very close, and the energy of the latter in the ground torsional state is only  $20\text{ cm}^{-1}$  higher than the corresponding energy of the trans-conformer.

For the HSSSH, DSSSH, and DSSSD molecules, the energies of the 30 lowest stationary torsional states were calculated, their symmetry species were determined in the  $C_{2v}(M)$  and  $C_s(M)$  molecular symmetry groups and their classification is performed based on the analysis of the corresponding wave functions, which makes it possible to identify the symmetric and antisymmetric fundamental torsional vibrations, their first and second overtones, as well as the number of combination torsional vibrations of molecules.

Torsional IR absorption spectra of the trans- and cis-conformers of three analyzed molecules at temperatures of 300 and 30 K were calculated. It was found that for the calculated torsional states, inter-conformational transitions are not present mainly due to the different spatial localization of the torsional wave functions of the trans- and cis-conformers. It was shown that for qualitative and quantitative analysis of the composition of the mixture of the HSSSH

conformers, one should use the symmetric torsional vibration of thiol groups in the trans-conformer ( $294\text{ cm}^{-1}$ ) and the antisymmetric torsional vibration of thiol groups in the cis-conformer ( $304\text{ cm}^{-1}$ ).

It has been established that the splitting of the ground vibrational state due to tunneling between equivalent configurations of trans-conformers in the HSSSH and DSSSD molecules is extremely small ( $2.2 \cdot 10^{-20}$  and  $7.5 \cdot 10^{-27}\text{ cm}^{-1}$ ). Such small value of the ground state energy splitting for the trisulfane molecule (which is still much smaller than the estimated in [12,13] splitting of the ground level due to the violation of parity law ( $10^{-12}\text{ cm}^{-1} \gg 10^{-20}\text{ cm}^{-1}$ )) give us hope for successful implementation of experiments which would observe the parity law violation in chiral molecules (see more arguments in [12]).

## 5. ACKNOWLEDGMENTS

This study was supported by the State Program of Scientific Investigations 2021-2025 “GPNI Convergence -25” (11.11.3).

## REFERENCES

- [1] F. Fehér, W. Laue, G. Winkhaus, Z.Anorg.Allgem.Chem., 228 (1956) 8.
- [2] E. Muller, J.B. Hyne, Can.J.Chem., 47 (1969) 1633-1637.
- [3] D. Cremer, J.Chem.Phys., 69 (1978) 4456-4471.
- [4] N. Colin Baird, J.Mol.Struct.(Theochem), 137 (1986) 1-8.
- [5] P. Birner, h.-J. Köhler, A. Karpfen, H. Lischka, J.Mol.Struct.(Theochem), 226 (1991) 223-8
- [6] D. Mauer, G. Winnerwisser, K.M.T. Yamada, J. Hahn, K. Reinartz, Z. Naturforsch., 43a (1988) 617-620.
- [7] D. Mauer, G. Winnerwisser, K.M.T. Yamada, J.Mol.Struct., 190 (1988) 457-464.
- [8] D. Mauer, G. Winnerwisser, K.M.T. Yamada, J.Mol.Spectr., 136 (1989) 380-386.
- [9] M. Liedtke, A.H. Saleck, K.M.T. Tamada, G. Winnerwisser, D. Cremer, E. Kraka, A. Dolgner, J. Hahn, S. Dobos, J.Phys.Chem., 97 (1993) 11204-11210.
- [10] M. Liedtke, K.M.T. Tamada, G. Winnerwisser, J. Hahn, J.Mol.Spectr., 413-414 (1997) 265-270.
- [11] M. Quack, Angew.Chem.Int.Engl., 28 (1989) 571-586.
- [12] C. Fábri, Ľ. Horný, M. Quack, ChemPhysChem, 16 (2015) 3584 - 3589
- [13] S. Albert, I. Bolotova, Z. Chen, C. Fábri, M. Quack, G. Seyfang, D. Zindel, Phys.Chem.Chem.Phys., 19 (2017) 11738.

- [14] R. Berger, M. Gottselig, M. Quack, M. Willeke, *Angew.Chem.Int.Ed.* 40 (2001) 4195-4198.
- [15] R. Berger, M. Gottselig, M. Quack, M. Willeke, *Angew.Chem.* 113 (2001) 4342-4345.
- [16] G.A. Pitsevich, A.Ye. Malevich, V.V. Sapeshko, The Hydroxyl Groups Internal Rotations in a Methanediol Molecule, *J.Mol.Spectr.*, 360 (2019) 31-38.
- [17] G.A. Pitsevich, A.E. Malevich, F.V. Markovich, U.U. Sapeshka, Barriers to internal rotation and tunnelling splittings of the torsional states in the HO(CH<sub>2</sub>)OH, DO(CH<sub>2</sub>)OH and DO(CH<sub>2</sub>)OD molecules, *Mol.Phys.*, 118 (2020) e1746425
- [18] G.A. Pitsevich, A.E. Malevich, U.U. Sapeshka, Torsional Spectrum of the Hydrogen Troxide Molecule, *Chem.Phys.*, 530 (2020) 110633.
- [19] G.A. Pitsevich, A.E. Malevich, D.G. Kisuryna, A.U. Vasilevsky, A.S. Vasilevich, U.U. Sapeshka, A.A. Kamnev, Quantum Aspects of Torsional Vibrations in the HO<sub>3</sub>H, DO<sub>3</sub>H, and DO<sub>3</sub>D Molecules, *Spectrochim.Acta Part A*, 239 (2020) 118209
- [20] G. Pitsevich, A. Malevich, V. Zheutok, A. Khrapunova, U. Sapeshka, Torsional Vibrations of Two Thiol Groups in the HSOSH, DSOSH, and DSOSD Molecule: 2D PES Study in CBS Limit, *Vib.Spectr.*, 113 (2021) 103208.
- [21] G. Pitsevich, A. Malevich, I. Doroshenko, Explicitly correlated study of the torsional vibrations of HSOSH molecule. Comparison with MP2/CBS(T,Q) level of theory, *Mol.Cryst.Mol.Liq.*, 749 (2022) 9 – 17.
- [22] G.A. Pitsevich, A.E. Malevich, D.G. Kisuryna, A.A. Ostyakov, U.U. Sapeshka, Torsional States and Tunneling Probability in HOSOH, DOSOD, and DOSOD Molecules Analyzed at the CBS Limit, *J.Phys.Chem. A* 124 (2020) 8733-8743.
- [23] G. Pitsevich, A. Malevich, Torsional motions of the free and H-bonded hydroxyl groups of the catechol molecule, *J.Mol.Spectr.*, 387 (2022) 111664
- [24] G.A. Pitsevich, A.E. Malevich, Features of the interaction of hydroxyl and methyl tops in the ethanol molecule: 2D-calculation of the torsion energy levels, *J.Appl.Spectr.*, 82 (2015) 540-553.
- [25] G.A. Pitsevich, A.E. Malevich, U.V. Lazicki, U.U. Sapeshka, The Torsional States of Methyl Hydroperoxide Molecule Calculated Using Anharmonic Zero Point Vibrational Energy, *Journal of the Belarusian State University. Physics*, 2 (2021) 15-24.
- [26] J.M. Bowman, S. Carter, X. Huang, *Int.Rev.Phys.Chem.* 22 (2003) 533.
- [27] W.D. Allen, A. Bodi. V. Szalay, A.G. Császár, *J.Chem.Phys.*, 124 (2006) 224310.
- [28] E. Mátyus, G. Czakó, B.T. Sutcliffe, A.G. Császár, *J.Chem.Phys.*, 127 (2007) 084102
- [29] J. Makarewicz, A. Skalożub, *Chem.Phys.Lett.*, 306 (1999) 352-356.
- [30] A. Fernández-Ramos, *J.Chem.Phys.*, 138 (2013) 134112

- [31] T.V. Alves, L. Simón-Carballido, F.R. Ornellas, A. Fernández-Ramos, PCCP 18 (2016) 8945-8953.
- [32] D. Ferro-Costas, M.N.D.S. Cordeiro, D.G. Truhlar, A. Fernández-Ramos, Comp. Phys. Comm., 232 (2018) 190-205.
- [33] M.L. Senent, Y.G. Smeyers, J.Mol.Struct. 464 (1999) 137-143.
- [34] T.J. Lukka, J.Chem.Phys., 102 (1995) 3945-3955.
- [35] S. Carter, N.C. Handy, 113 (2000) 987-993.
- [36] S. Carter, A.R. Sharma, J.M. Bowman, J.Chem.Phys., 135 (2011) 014308
- [37] M. J. Frisch, G. W. Trucks, H. B. Schlegel, G. E. Scuseria, M. A. Robb, J. R. Cheeseman, G. Scalmani, V. Barone, B. Mennucci, G. A. Petersson, H. Nakatsuji, M. Caricato, X. Li, H. P. Hratchian, A. F. Izmaylov, J. Bloino, G. Zheng, J. L. Sonnenberg, M. Hada, M. Ehara, K. Toyota, R. Fukuda, J. Hasegawa, M. Ishida, T. Nakajima, Y. Honda, O. Kitao, H. Nakai, T. Vreven, J. Montgomery, J. A., J. E. Peralta, F. Ogliaro, M. Bearpark, J. J. Heyd, E. Brothers, K. N. Kudin, V. N. Staroverov, R. Kobayashi, J. Normand, K. Raghavachari, A. Rendell, J. C. Burant, S. S. Iyengar, J. Tomasi, M. Cossi, N. Rega, N. J. Millam, M. Klene, J. E. Knox, J. B. Cross, V. Bakken, C. Adamo, J. Jaramillo, R. Gomperts, R. E. Stratmann, O. Yazyev, A. J. Austin, R. Cammi, C. Pomelli, J. W. Ochterski, R. L. Martin, K. Morokuma, V. G. Zakrzewski, G. A. Voth, P. Salvador, J. J. Dannenberg, S. Dapprich, A. D. Daniels, C. Farkas, J. B. Foresman, J. V. Ortiz, J. Cioslowski, D. J. Fox, *Gaussian 09, Revision A.1*, Gaussian, Inc., Wallingford CT (2009).
- [38] G. Hetzer, P. Pulay, H.J. Werner, Chem. Phys. Lett. 290 (1998) 143–149.
- [39] M. Schutz, G. Hetzer, H.J. Werner., J. Chem. Phys. 111 (1999) 5691–5705.
- [40] R.A. Kendall, T.H. Dunning, R.J. Harrison, J. Chem. Phys. 96 (1992) 6796–6806.
- [41] D.E. Woon, T.H. Dunning Jr., J. Chem. Phys. 98 (1993) 1358–1371.
- [42] T.H. Dunning Jr., J. Chem. Phys. 90 (1989) 1007.
- [43] A.D. Becke, J.Chem.Phys., 98 (1993) 5648.
- [44] C. Lee, W. Yang, R.G. Parr, Phys.Rev., B 37 (1988) 785
- [45] P.J. Stephens, F.J. Devlin, C.F. Chabalowski, M.J. Frisch, J.Phys.Chem., 98 (1994) 11623
- [46] T.H. Dunning Jr., J.Chem.Phys. 90 (1989) 1007-1023.
- [47] R.A. Kendall, T.H. Dunning Jr., R.J. Harrison, J.Chem.Phys., 96 (1992) 6796-6806.
- [48] D.E. Woon, T.H. Dunning Jr., J.Chem.Phys., 98 (1993) 1358-1371.
- [49] K. Raghavachari, G.W. Trucks, J.A. Pople, M. Head-Gordon, Chem. Phys. Lett. 157 (1989) 479.
- [50] G.E. Scuseria, J. Chem. Phys. 94 (1991) 442–447.

- [51] A. Halkier, T. Helgaker, P. Jorgensen, W. Klopper, H. Koch, J. Olsen, A.K. Wilson, Chem.Phys.Lett., 286 (1998) 243-252.
- [52] M. Okoshi, T. Atsumi, H. Nakai, J.Comp.Chem., 36 (2015) 1075-1082.
- [53] E.B. Wilson, J.J.C. Decius, P.C. Cross, Molecular Vibration. Dover Publications, Inc., New York, 1955
- [54] C. Lanczos, Discourse on Fourier Series, Oliver and Boyd Ltd, Edinburgh and London, 1966
- [55] G.A. Pitsevich, A.E. Malevich, Optics and Photonic Journal, 2 (2012) 332-337
- [56] Mathematica, Wolfram Research, Inc., <http://www.wolfram.com/mathematica>
- [57] J.M. Flaud, C. Camy-Peyret, J.Mol.Spectr., 55 (1975) 278
- [58] W. Gordy, R.L. Cook, Microwave Molecular Spectra, Interscience Publishers, 1970
- [59] G. Duxbury, Infrared Vibration-Rotation Spectroscopy, John Wiley & Sons LTD, 2000
- [60] P. R. Bunker and P. Jensen, Molecular Symmetry and Spectroscopy, NRC Research Press, Ottawa (1998).
- [61] Carlo Di Lauro, Rotational Structure in Molecular Infrared Spectra, Elsevier, 2013.
- [62] G. Pitsevich, E. Shalamberidze, A. Malevich, V. Sablinskas, V. Balevicius, L.G.M. Pettersson, Calculation of the Vibration-Rotational Transition Intensities of Water Molecules Trapped in a Argon Matrix: Stretching O-H Vibrations Spectral Region, Mol.Phys., 115 (2017) 2605-2613.